Laboratory evolution of *E. coli* with a natural vitamin B_{12} analog reveals roles for cobamide uptake and adenosylation in methionine synthase-dependent growth

Kenny C. Mok, Zachary F. Hallberg, Rebecca R. Procknow, and Michiko E. Taga[#]

Department of Plant & Microbial Biology, University of California, Berkeley, Berkeley, CA U.S.A.

[#]Correspondence to taga@berkeley.edu

Running title: Lab evolution with pseudocobalamin

Abstract

Bacteria encounter chemically similar nutrients in their environment that impact their growth in distinct ways. Among such nutrients are cobamides, the structurally diverse family of cofactors related to vitamin B_{12} (cobalamin), which function as cofactors for diverse metabolic processes. Given that different environments contain varying abundances of different cobamides, bacteria are likely to encounter cobamides that enable them to grow robustly as well as those that do not function efficiently for their metabolism. Here, we performed a laboratory evolution of a cobamide-dependent strain of *Escherichia coli* with pseudocobalamin (pCbl), a cobamide that *E. coli* uses less effectively than cobalamin for MetH-dependent methionine synthesis, to identify genetic adaptations that lead to improved growth with less-preferred cobamides. After propagating and sequencing nine independent lines and validating the results by constructing targeted mutations, we found that mutations that increase expression of the outer membrane cobamide transporter BtuB are beneficial during growth under cobamide-limiting conditions. Unexpectedly, we also found that overexpression of the cobamide adenosyltransferase BtuR confers a specific growth advantage in pCbl. Characterization of the latter phenotype revealed that BtuR and adenosylated cobamides contribute to optimal MetH-dependent growth. Together, these findings improve our understanding of how bacteria expand their cobamide-dependent metabolic potential.

Importance

In nature, bacteria commonly experience fluctuations in the availability of required nutrients. Thus, their environment often contains nutrients that are insufficient in quantity or that function poorly in their metabolism. Cobamides, the vitamin B_{12} family of cofactors, are ideal for investigating the influence of nutrient quality on bacterial growth. We performed a laboratory evolution experiment in *E. coli* with a less-preferred cobamide to examine whether and how bacteria can improve their growth with less ideal nutrients. We found that overexpression of genes for cobamide uptake and modification are genetic adaptations that improve growth under these conditions. Given that cobamides are key shared metabolites in microbial communities, our results reveal insights into bacterial interactions and competition for nutrients.

Introduction

Cobamides, the vitamin B_{12} family of metabolites, are used by most bacteria as cofactors for diverse metabolic processes including carbon metabolism, synthesis of methionine and deoxyribonucleotides, and natural product biosynthesis (1). They are produced exclusively by prokaryotes, though most bacteria that use cobamides are incapable of *de novo* synthesis (2, 3). Cobamides are modified tetrapyrroles (corrinoids) with a central cobalt ion that can coordinate to variable upper and lower axial ligands (2). The upper (β) ligand varies depending on catalytic function: a 5′-deoxyadenosyl group is used for radical-based molecular rearrangements, while a methyl group is used for methyltransfer reactions (Fig. 1A). While B_{12} (cobalamin, Cbl) (Fig. 1A) is the best-studied cobamide due to its importance in human health (4), nearly 20 other cobamides with structural variability in the lower (α) axial ligand have been described (5-7). Different cobamides have distinct effects on microbial growth because cobamide-dependent growth and enzyme function are differentially impacted by lower ligand structure (6, 8-15). Diverse assortments of cobamides have been found in microbial communities from host-associated and environmental sources, and variability in cobamide abundances has been observed even in samples derived from similar sources (5, 16, 17). Recent studies have shown that microbial community composition can be significantly altered by addition of certain cobamides, suggesting cobamides can influence microbiomes (18-22). Because microbes can be exposed to different cobamides as their environments shift, they may encounter cobamides that function at varying levels of effectiveness for their metabolism. Given that cobamide structure and availability impact bacterial fitness and community structure, it is important to understand how bacteria are genetically wired to deal with different cobamides.

Many organisms have evolved strategies to cope with the absence of preferred cobamides. Certain bacteria, archaea, and algae carry out cobamide remodeling, whereby non-preferred cobamides are converted into forms that can be used by their cobamide-dependent enzymes (9, 23-27). In addition, many bacteria encode cobamide-independent alternative enzymes or pathways, circumventing the need for cobamides for certain processes (3, 28). For example, cobamide-independent methionine synthase (MetE) and ribonucleotide reductases are each found in over half of bacterial genomes, including in approximately 80 and 40% of genomes that encode cobamide-dependent counterparts to these enzymes, respectively (3). Bacteria can also tailor their genetic response to the cobamides they prefer via selectivity in riboswitches, noncoding RNA elements in the 5′ untranslated region (UTR) of mRNA that, upon binding to specific cobamides, typically downregulate expression of cobamide biosynthesis enzymes, transporters, and cobamide-independent enzymes (29-32).

Here, we carried out a laboratory evolution experiment in *Escherichia coli* to investigate whether there are additional genetic strategies microbes may employ to improve their use of less-preferred cobamides. Due to its short generation time and genetic tractability, *E. coli* is used extensively as a model system to address fundamental biological questions. Although *E. coli* does not require exogenous cobamides in the absence of methionine because it contains *metE*, a Δ*metE* mutant relies on the cobamide-dependent methionine synthase MetH. Adeninylcobamide (pseudocobalamin, pCbl) (Fig. 1A) is a cobamide present in diverse environments, such as the human gut (16), but we find it is used less effectively than Cbl by *E. coli*. In our evolution experiment, we found that, indeed, an *E. coli* Δ*metE* mutant can improve its growth with pCbl via several genetic strategies. Different sets of mutations were found in evolved lines provided with

84 different pCbl concentrations, but a common strategy that emerged was increasing the expression
85 of the outer membrane corrinoid transporter BtuB by 300-fold, which provided a competitive
86 advantage in limiting concentrations of cobamides. We additionally found that evolved lines and
87 engineered strains that overexpress the corrinoid adenosyltransferase BtuR are better adapted for
88 growth on pCbl. As a result, this study has revealed a previously unknown role for BtuR in MetH-
89 dependent growth.

90 **Results**

91 *Laboratory evolution of* E. coli *improves use of pCbl during MetH-dependent growth*

92 The *E. coli* MG1655 Δ*metE* strain, which requires MetH activity for growth in minimal
93 medium lacking methionine, prefers Cbl over pCbl, as revealed by comparing growth with the two
94 cobamides (Fig. 1B). Specifically, the concentration of pCbl necessary for half-maximal growth
95 (EC_{50}) of this strain is over 10-fold higher than for Cbl, and the maximal growth yield (OD_{600}) is
96 lower with pCbl (Fig. 1B). We therefore performed a laboratory evolution experiment with pCbl
97 to determine whether *E. coli* can improve its use of this less-preferred cobamide. Nine independent
98 cultures of the *E. coli* Δ*metE* strain were passaged daily for 104 days for a total of approximately
99 700 generations in M9 minimal medium containing either 0.75, 0.55, or 0.35 nM pCbl (Fig. 1C).
100 These concentrations encompassed nearly-saturating to limiting growth of the ancestral strain (Fig.
101 1B). Five of the nine cultures reached a maximal OD_{600} below 0.6 during some or all of the first
102 10 days, but exceeded an OD_{600} of 1.2 for nearly all passages after day 30, indicating they had
103 adapted to the limiting pCbl conditions (Fig. 1C). When compared to the ancestor, all nine

populations showed improved growth with 0.35 nM pCbl (Fig. 1D). The nine populations also showed improved growth with Cbl (Fig. 1E), suggesting that they had evolved better use of

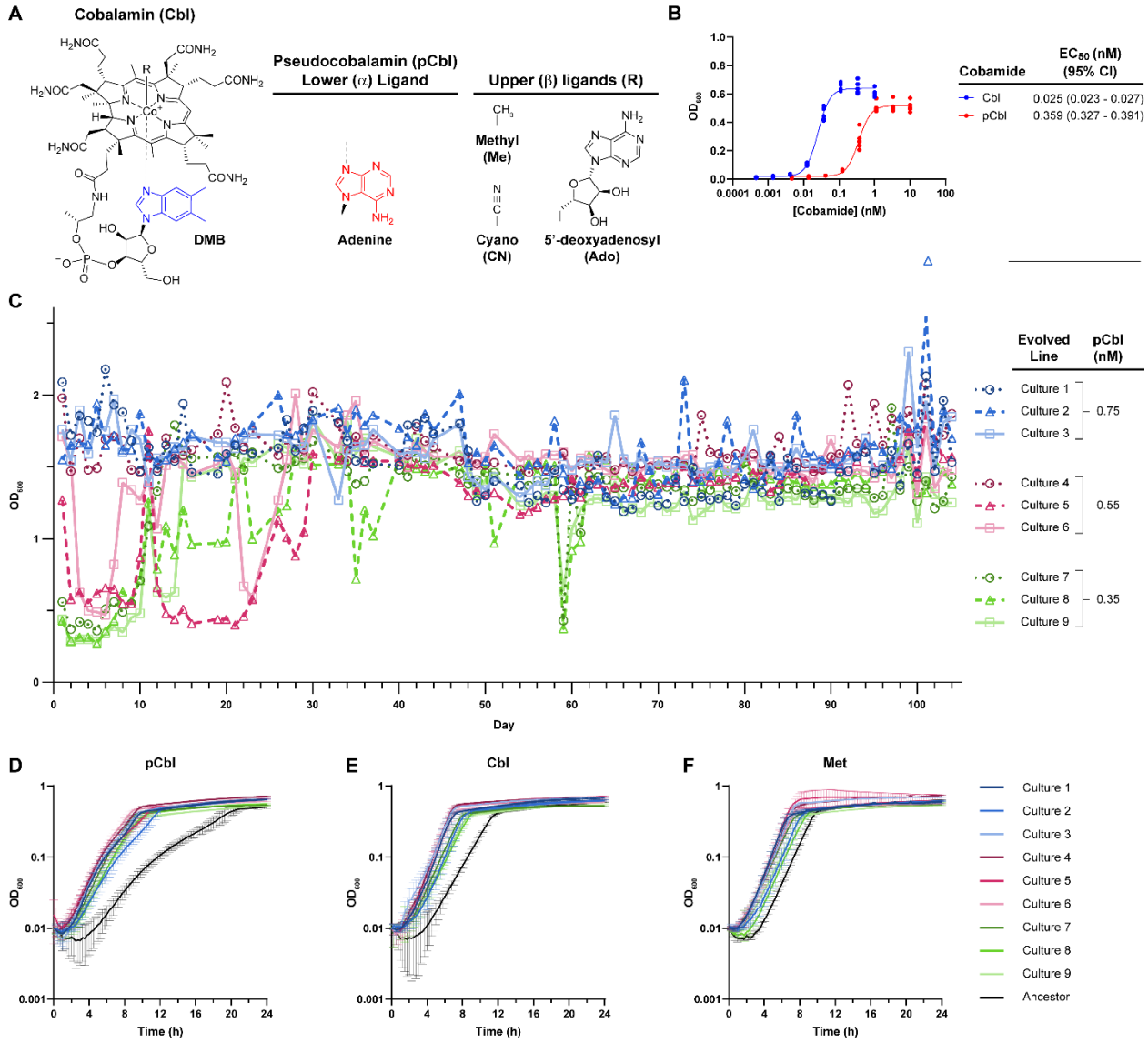

Figure 1. Laboratory evolution of *E. coli* improves its growth with pCbl. A) Structure of cobalamin (Cbl; B_{12}) with its lower ligand 5,6-dimethylbenzimidazole (DMB) in blue. Pseudocobalamin (pCbl) contains adenine (red) as its lower ligand. Cobamide upper ligands characterized in this study are shown. B) Dose-response curves of *E. coli* Δ*metE* grown in the absence of methionine with various concentrations of Cbl or pCbl. OD_{600} was recorded after 22 hours. EC_{50} values and 95% confidence intervals of six biological replicates for each cobamide are shown. C) Growth of *E. coli* Δ*metE* cultures during laboratory evolution. Three biological replicate cultures of *E. coli* Δ*metE* were passaged daily in M9 medium supplemented with 0.75, 0.55, or 0.35 nM pCbl for 104 days. OD_{600} was measured prior to diluting 1:100 into fresh medium every 24 hours. D-F) Growth curves of evolved populations (Day 104) and the ancestral Δ*metE* strain in media with 0.35 nM pCbl (D), 0.35 nM Cbl (E), or 0.1 mg/ml Met (F). The average of three biological replicates is shown for panels D-F; error bars represent standard deviation.

cobamides in general. Growth with Met was modestly improved in the evolved populations, indicating they had adapted to other features of the growth medium (Fig. 1F).

Mutants in one evolved population have a growth advantage specifically with pCbl

We noticed that, when plated on LB agar, which contains methionine, some of the colonies from a passaged culture containing 0.35 nM pCbl (Culture 8) were distinctly smaller than the others (Fig. 2A). These small-colony variants first appeared on day 28, and they made up nearly the whole population on day 65 before being almost entirely lost by day 84 (Fig. 2B). Small-colony variants can arise during laboratory evolution experiments and often are not related to the phenotype being studied, as is the case in this study (see below) (33). Nonetheless, we took advantage of this distinct morphology by using it as a convenient markerless phenotype for further characterizing the pCbl-specific growth advantage of these strains.

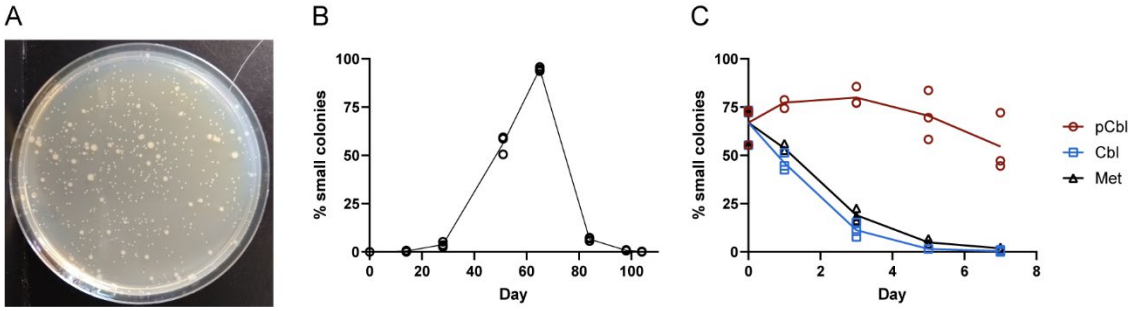

Figure 2. Small colony variants emerge during evolution of Culture 8. A) Plating of a population of Culture 8 on LB agar shows the regular and small colony phenotypes. B) The percentage of total colonies with small size was determined for archived populations of Culture 8. The Δ*metE* ancestor was used for the zero timepoint. C) The percentage of small colonies is plotted for the day 65 archived population of Culture 8 grown with 0.35 nM pCbl, 0.35 nM Cbl, or 0.1 mg/ml Met over seven days with daily passaging. Lines connect the means of three biological replicates.

Growth experiments on the archived culture from day 65 showed that the small-colony variants persisted following one week of daily passaging in the presence of pCbl, whereas their abundance decreased to zero in media containing Cbl or Met (Fig. 2C). The percentage of small colonies in the cultures supplemented with pCbl started to decrease on day 5 of the experiment (Fig. 2C), suggesting that the same population dynamics may have been occurring that were seen during the laboratory evolution (Fig. 2B).

We isolated colonies with different sizes from the day 65 population and individually competed three "small" isolates (S2, S3, and S4) against two "regular" isolates (R1 and R3), as well as the ancestral Δ*metE* strain, in media containing either pCbl, Cbl, or Met. All three small isolates had similar phenotypes. When co-cultured, the small isolates outcompeted the ancestor in the presence of cobamides, taking over the entire population after a single passage with pCbl and after three passages with Cbl (Fig. 3A, B, Fig. S1 A, B, D, E). In media with methionine, however, the ancestral strain outcompeted the evolved isolates (Fig. 3C, Fig. S1 C, F). When the small isolates were competed against the two regular isolates, the small isolates were outcompeted when grown with Cbl and Met, but we observed contrasting phenotypes with pCbl (Fig. 3 A-C, Fig. S1). The small isolates had a competitive advantage over regular isolate R1 but were outcompeted by R3 (Fig. 3A, Fig. S1 A, D).

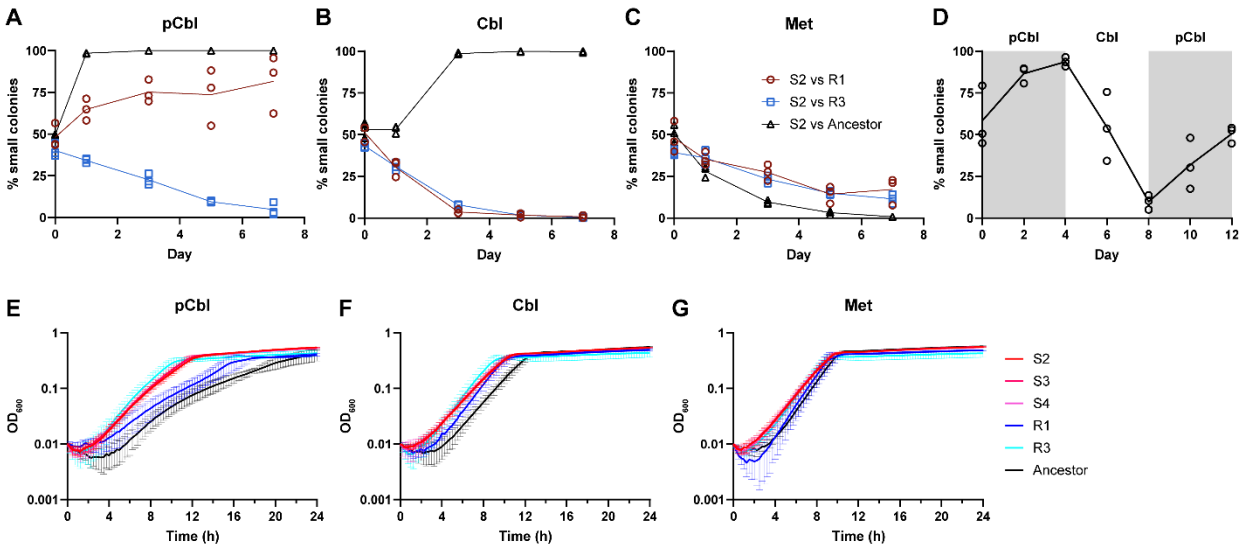

Figure 3. Growth characteristics of isolates S2, R1, and R3 from Culture 8. A-C) Isolate S2 was competed against isolates R1 and R3 and the ancestor strain for seven days with daily passaging in medium containing 0.35 nM pCbl (A), 0.35 nM Cbl (B), or 0.1 mg/ml Met (C). Cultures were diluted and plated on the indicated days to quantify the fraction of small colonies, corresponding to S2 strain abundance. D) Isolates S2 and R1 were competed for 12 days with daily passaging in medium containing either 0.35 nM pCbl (shaded) or 0.35 nM Cbl (unshaded), and the fraction of small colonies (S2) was calculated as in panels A-C. Lines in A-D connect the means of three biological replicates. E-G) Growth curves of isolates S2, S3, S4, R1, R3 and the ancestor strain in media containing 0.35 nM pCbl (E), 0.35 nM Cbl (F), or 0.1 mg/ml Met (G). The average of three biological replicates is shown; error bars represent standard deviation.

The competitive advantage of the small isolates with pCbl was further confirmed by co-culturing isolates S2 and R1 in medium supplemented alternately with pCbl and Cbl. When passaged with pCbl for four days, the proportion of S2 increased to over 90%, but after switching to the Cbl-containing medium, the proportion of S2 decreased to less than 10% after four days. A subsequent return to pCbl resulted in an increase in S2 (Fig. 3D).

The phenotypes of the small and regular isolates that we observed in competition were consistent with their growth characteristics in pure culture (Fig. 3E-G). Isolates S2, S3, and S4, which outcompeted the ancestor in media with pCbl and Cbl but were outcompeted with Met, grew faster than the ancestor in the presence of cobamides while showing a small growth improvement with Met (Fig. 3E-G). Only isolate R1, which competed poorly in the presence of pCbl, had less improved growth than the other isolates, particularly in the medium containing pCbl (Fig. 3E). Isolate R3, which outcompeted the small isolates in all three media conditions, grew similarly to the small isolates in each medium (Fig. 3E-G). Taken together, these results suggest that all of the isolates have acquired one or more mutations that confer a growth advantage with cobamides. Further, based on the growth phenotypes of strains S2, S3, S4 and R3 with pCbl, these strains likely have one or more mutations that confer a specific advantage with pCbl.

151 *Evolved isolates have mutations that increase expression of cobamide-related genes*

152 To identify the mutations acquired during the evolution experiment, we performed whole
153 genome sequencing on the isolates from Culture 8. Each isolate has a unique set of mutations,
154 which range from 8 to 14 single nucleotide polymorphisms (SNPs), insertions and deletions
155 (InDels), or structural variants (SVs) (Fig. 4A; Table S1). This includes mutations in known

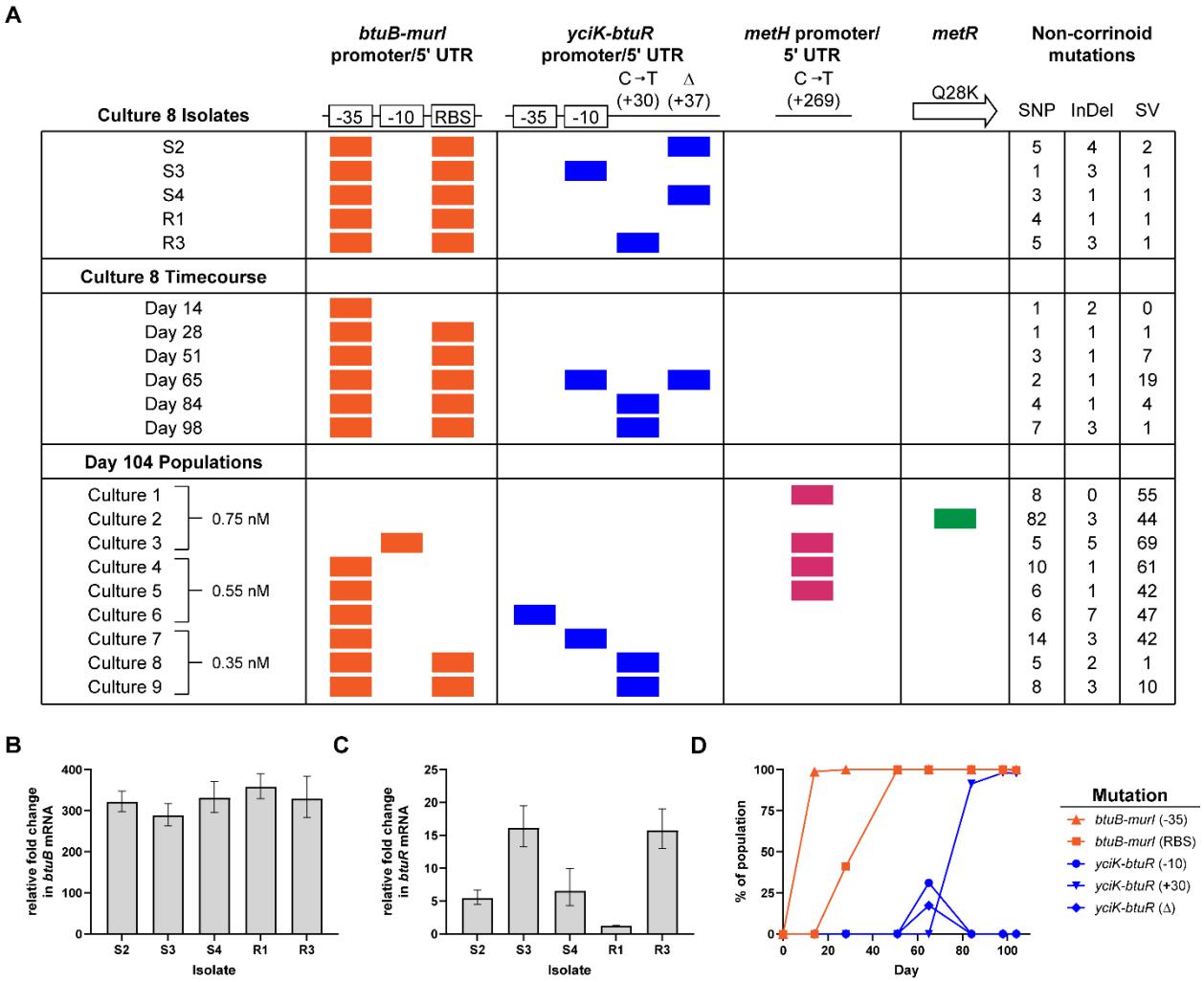

Figure 4. Corrinoid-related genes are mutated and upregulated during evolution. A) Colored boxes show the presence of the indicated mutations affecting corrinoid-related genes in isolates and archived timepoints from Culture 8, and in the endpoint (Day 104) populations of all evolved lines. The promoter for the *yciK-btuR* operon has not been experimentally characterized and was predicted by PromoterHunter (67). The specific changes in the promoters and 5′ UTRs of *btuB-murI* and *yciK-btuR* are shown in Figure S2. *yciK-btuR* is on the minus strand of the chromosome and the +30 change (C to T) is the reverse complement of the mutation in the 5′ UTR. The concentration of pCbl present during the evolution of each line (Cultures 1-9) is indicated. The numbers of SNPs, InDels, and SVs affecting non-corrinoid-related genes in each sequenced isolate or population are shown (see Table S1 for list of genes and mutations). B-C) *btuB* (B) and *btuR* (C) transcript levels in evolved isolates relative to Δ*metE* ancestor from cultures containing 1 nM pCbl as determined by RT-qPCR. Mean and error were calculated from three biological replicates. D) Frequency of the *btuB-murI* and *yciK-btuR* mutations within the Culture 8 population during the evolution experiment.

156 cobamide-related genes in all five isolates. They each have the same two SNPs in the promoter
157 and ribosome binding site (RBS) of the *btuB-murI* operon, which encodes the outer membrane
158 corrinoid transporter BtuB and the glutamate racemase MurI (Fig. 4A). We predict that these
159 mutations result in increased expression of the operon (see Fig. S2A for details). RT-qPCR on the
160 ancestor strain and the evolved isolates confirmed that the operon is overexpressed in the evolved
161 isolates. *btuB-murI* transcript levels in the evolved isolates were approximately 300-fold higher
162 than in the ancestor (Fig. 4B).

163 In addition to the mutations in *btuB-murI*, all of the isolates except R1 have a mutation in
164 the predicted promoter or 5′ UTR of the *yciK-btuR* operon (Fig. 4A, Fig. S2B). *yciK* is an
165 uncharacterized gene annotated as a putative oxidoreductase, and *btuR* encodes an
166 adenosyltransferase that installs a 5′-deoxyadenosyl group as the β ligand of corrinoids. RT-qPCR
167 analysis of the evolved isolates showed that isolates with *btuR* mutations (S2, S3, S4, and R3) had
168 5- to 15-fold higher levels of *yciK-btuR* mRNA compared to the ancestor, while mRNA levels
169 similar to the ancestor were observed in isolate R1, which does not have a mutation in *yciK-btuR*
170 Fig. 4B). These results suggest that growth of *E. coli* with limiting amounts of pCbl can be
171 improved by increasing the expression of these two operons.

172 Sequencing of the archived populations of Culture 8 enabled us to follow the emergence
173 of these mutations during the evolution experiment (Fig. 4A, D; Table S1). Both *btuB-murI*
174 mutations arose early in the timecourse and were retained within the entire population by day 51
175 (Fig. 4D). Notably, mutations in the -35 element and RBS were present by days 14 and 28,
176 respectively, coinciding with increases in the OD_{600} of the culture (Fig. 1C).

177 The two *yciK-btuR* mutations found in the small isolates were first detected on day 65, in
178 31 and 17% of the population, respectively (Fig. 4D). At all of the following timepoints, however,
179 only the C to T mutation found in isolate R3 was detected in the population. Given that isolate R3
180 outcompeted isolates S2, S3 and S4 in pCbl (Fig. 3A, Fig. S1), it is likely that descendants of R3
181 became dominant in the population after day 65. An *rpsK* mutant was observed to have a small
182 colony phenotype in a previous study in *E. coli* (34), and we found here that the frequency of an
183 *rpsK* mutation correlated with the prevalence of small colonies in the population (Table S1).

184 E. coli *adapts differently with limiting versus near-saturating pCbl*

185 The endpoint (Day 104) archives of the nine evolved cultures were also sequenced. The
186 populations have several of the cobamide-associated mutations found in the Culture 8 isolates and
187 earlier timepoints, as well as mutations in nearly 400 additional genes, including 75 genes found
188 mutated in more than one sample (Fig. 4A; Table S1). In each population, at least one known
189 cobamide-related gene is mutated, with different genes affected depending on the concentration of
190 pCbl present during the evolution (Fig. 4A). The two other populations passaged with 0.35 nM
191 pCbl developed the same mutations upstream of *btuB-murI* and *yciK-btuR* as those found in
192 Culture 8 (Fig. 4A, Cultures 7 and 9). In contrast, only a minor fraction (14%) of one population
193 passaged with 0.75 nM pCbl has a mutation upstream of *btuB-murI*, and one population passaged
194 with 0.55 nM pCbl has a mutation upstream of *yciK-btuR* (Cultures 3 and 6, respectively; Fig. 4A;
195 Table S1), though all three populations grown with 0.55 nM pCbl have the same *btuB-murI*
196 promoter mutation found in the isolates.

All of the evolved populations lacking mutations in *yciK-btuR* have a mutation upstream of *metH* or in the coding sequence of *metR*, a transcriptional activator of *metH* (35), in 50% or more of the population (Culture 1-5; Fig. 4A; Table S1). It is unclear how these mutations affect *metH* expression; the *metH* mutation is not located in the promoter, RBS, or MetR binding site (36), while the *metR* mutation is located in its DNA-binding domain (37). Taken together, these results suggest that increasing cobamide uptake and adenosylation are effective strategies for improving growth with limiting to moderate pCbl concentrations, while changing expression of *metH* facilitates adaptation at higher concentrations of pCbl.

Overexpression of the corrinoid uptake gene btuB *is advantageous at limiting cobamide concentrations*

Having found that the operons containing *btuB* and *btuR* are upregulated in the evolved isolates, we next examined how overexpression of each gene separately affects cobamide-dependent growth. We first investigated the influence of *btuB* alone, since the glutamate racemase MurI, encoded in the same operon, has no known function in cobamide metabolism (38). We constructed a strain with a Δ*metE* mutation that overexpresses *btuB* by inserting a second copy of the gene into the chromosome, with its promoter containing the G to T mutation found in the -35 element of the evolved isolates. This strain was competed against a Δ*metE* control strain, with each strain expressing either CFP or YFP to monitor their abundances in co-culture. We found that overexpression of *btuB* conferred a competitive advantage in media containing 1 nM pCbl, but not

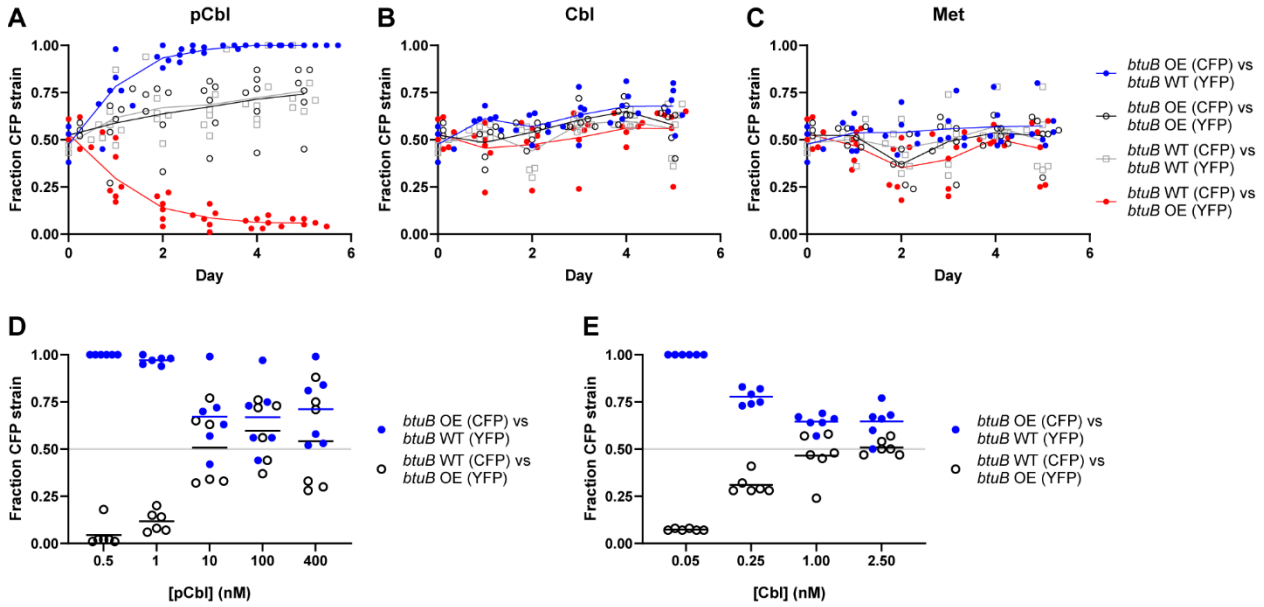

Figure 5. Overexpression of *btuB* confers a competitive advantage at limiting cobamide concentrations. A-C) *E. coli* Δ*metE* strains overexpressing *btuB* (OE) or producing native levels of *btuB* (WT), each expressing either CFP or YFP, were competed in co-culture for five days with daily passaging in medium containing either 1 nM pCbl (A), 1 nM Cbl (B), or 0.1 mg/ml Met (C). The fraction of the CFP-expressing strain in each co-culture is plotted. Control co-cultures containing CFP- and YFP-expressing strains in the same genetic background (black and gray) were included to rule out a growth disadvantage caused by either fluorescent protein. D-E) The CFP- and YFP-expressing strains that overexpress *btuB* (OE) or produce native levels of *btuB* (WT) were competed in co-culture at different concentrations of pCbl (D) or Cbl (E). Fluorescence was measured on day 3 following daily passaging. Lines represent the means of six biological replicates.

216 1 nM Cbl or Met (Fig. 5 A-C). However, competing the strains in varying cobamide concentrations
217 showed that *btuB* overexpression is beneficial with both pCbl and Cbl, but only at concentrations
218 at which the cobamide is limiting, namely 1 nM and less for pCbl, and under 0.25 nM for Cbl (Fig.
219 5D, E). Thus, the *btuB* mutations that arose during passaging with limiting pCbl presumably
220 improved *E. coli*'s ability to import cobamides to support MetH-dependent growth.

221 *The corrinoid adenosyltransferase gene* btuR *is required for optimal MetH-dependent growth*

222 Next, we assessed whether increasing *btuR* expression impacts MetH-dependent growth
223 by overexpressing *btuR* on a plasmid. We found that, similar to the results with *btuB*, a strain
224 overexpressing *btuR* outcompeted a strain with wild type *btuR* levels when grown with pCbl, but
225 not with Cbl or Met (Fig. 6 A-C). Though it is in an operon with *yciK*, *btuR* alone was responsible
226 for this phenotype, as overexpression of *yciK* did not confer a growth advantage with pCbl and co-
227 expression of *yciK* with *btuR* did not influence the effect of overexpression of *btuR* alone (Fig.
228 S3). However, unlike *btuB*, overexpression of *btuR* conferred a competitive growth advantage even
229 at concentrations of up to 400 nM pCbl, but failed to confer an advantage at any concentration of
230 Cbl tested (Fig. 6 D, E).

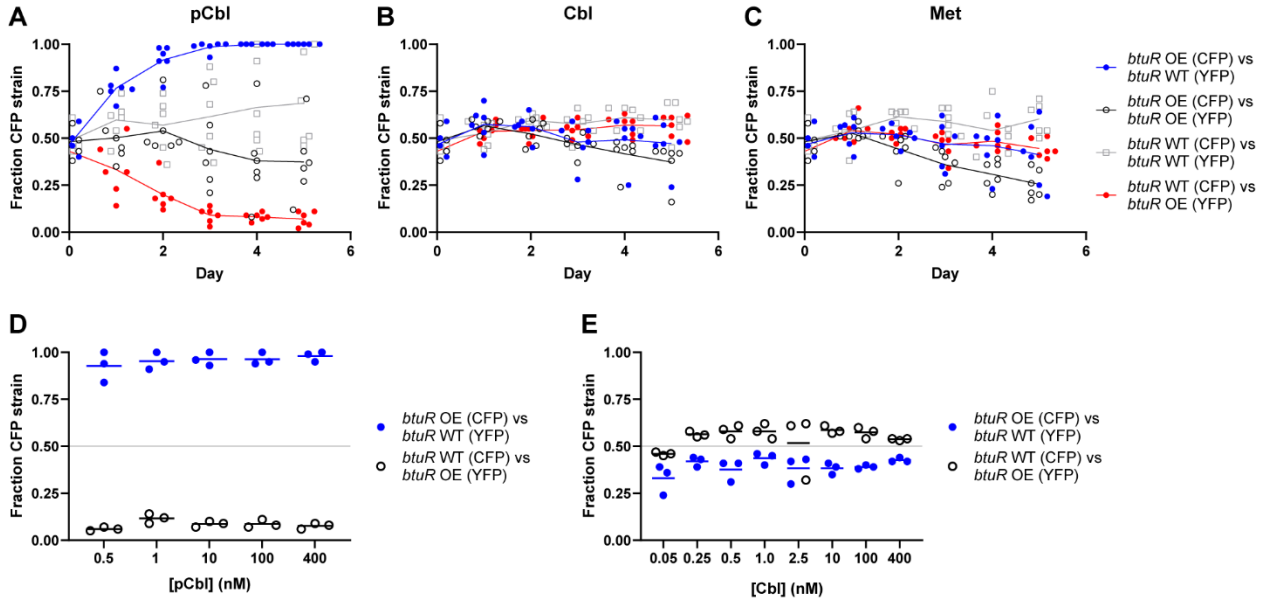

Figure 6. Overexpression of *btuR* confers a competitive advantage only during growth with pCbl. A-C) *E. coli* Δ*metE* strains overexpressing *btuR* (OE) or producing native levels of *btuR* (WT), each expressing CFP or YFP, were competed in co-culture for five days with daily passaging in medium containing either 1 nM pCbl (A), 1 nM Cbl (B), or 0.1 mg/ml Met (C). The fraction of the CFP-expressing strain in each co-culture is plotted. Control co-cultures containing CFP- and YFP-expressing strains in the same genetic background (black and gray) were included to rule out a growth disadvantage caused by either fluorescent protein. D-E) The CFP- and YFP-expressing strains that overexpress *btuR* (OE) or produce native levels of *btuR* (WT) were competed in co-culture at different concentrations of pCbl (D) or Cbl (E). Fluorescence was measured on day 3 following daily passaging. Lines represent the means of six biological replicates.

231 In the Δ*metE* mutant, cobamides are used by the MetH enzyme to transfer methyl groups
232 from methyltetrahydrofolate to homocysteine by alternately methylating and demethylating the
233 cobamide at the β position. It was therefore puzzling to find that overexpression of BtuR, which
234 adenosylates cobamides at the β position, improves MetH-dependent growth. To further explore

235 the role of BtuR in MetH-dependent growth, we deleted *btuR* and performed growth assays with
236 pCbl or Cbl with either cyano (CN, as in Fig. 1-6) or adenosyl (Ado) β ligands (Fig. 1A). Growth
237 measurements with these cobamides showed that a Δ*btuR* Δ*metE* strain has impaired growth in
238 cyanopseudocobalamin (CNpCbl), with a lower maximum OD_{600} and an EC_{50} over 25-fold higher
239 than the Δ*metE* strain (Fig. 7A). Growth with adenosylpseudocobalamin (AdopCbl) led to a higher
240 maximum OD_{600} and lower EC_{50} of the Δ*btuR* Δ*metE* strain, though growth was still considerably
241 impaired compared to the Δ*metE* strain (Fig. 7A). A similar trend was observed when these strains
242 were cultured with cyanated versus adenosylated forms of Cbl (CNCbl and AdoCbl, respectively),
243 though the growth impairment of the Δ*btuR* Δ*metE* strain was more modest (Fig. 7B). Together,
244 these results confirm that *btuR* influences MetH-dependent growth in *E. coli.*

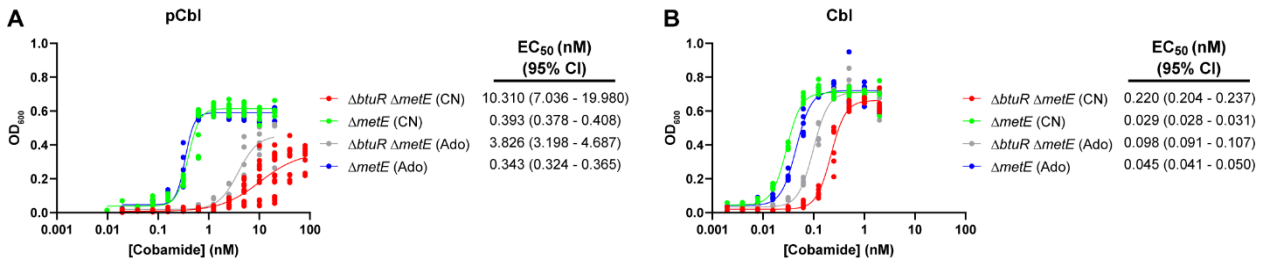

Figure 7. Deletion of *btuR* causes poorer growth with pCbl and Cbl. A-B) Cobamide dose-response curves are shown for *E. coli* Δ*btuR* Δ*metE* and Δ*metE* strains grown with various concentrations of CNpCbl and AdopCbl (A), or CNCbl and AdoCbl (B) with no added methonine. OD_{600} was recorded after 22 hours of growth. EC_{50} values and 95% confidence intervals were calculated from 6-18 biological replicates for each cobamide concentration.

245

246 The growth defect of the Δ*btuR* Δ*metE* strain and partial rescue by adenosylated cobamides
247 could be due to differences in cobamide uptake or retention. To examine this possibility, we
248 measured the amount of cobamide in the supernatant and cell pellet fractions in the Δ*btuR* Δ*metE*
249 and Δ*metE* strains cultured with each of the four cobamides tested in Figure 7 (AdopCbl, CNpCbl,
250 AdoCbl, CNCbl) using a quantitative bioassay that detects corrinoids (cobamides and biosynthetic
251 precursors). Strains lacking *btuR* had approximately twofold less AdopCbl and CNpCbl in the cell
252 pellet fraction (Fig. S4A); this result was validated by HPLC analysis of corrinoid extractions (Fig.
253 S4D). No differences in the levels of either AdoCbl or CNCbl was observed between the Δ*btuR*
254 Δ*metE* and Δ*metE* strains, but less AdoCbl was found in the cell pellets than CNCbl (Fig. S3 B,
255 C). The twofold differences in intracellular pCbl levels between the strains may only partially
256 explain the 10- to 25-fold differences in EC_{50} and differences in maximal OD_{600} observed in the
257 dose-response assays (Fig. 7A). Thus, it is possible that the adenosylated forms of cobamides play
258 a previously unrecognized role in promoting MetH activity.

259 **Discussion**

260 Cobamides are considered key shared nutrients because they function as cofactors for
261 numerous microbial processes but are only produced by a subset of prokaryotes. They have been
262 detected in diverse microbial communities, both environmental and host-associated, and a wide
263 range in cobamide levels has been observed across ecosystems, with some dominated by one or
264 two cobamides, while others contain up to eight different types (16). These differences in

265 cobamide diversity across environments are noteworthy in light of the observation that many
266 bacteria have preferences for particular cobamides and most bacteria rely on cobamides produced
267 by other microbes. This raises the question of how bacteria adapt in the presence of non-preferred
268 cobamides. We addressed this question by using a cobamide-dependent mutant of *E. coli* in a
269 laboratory evolution experiment. We found that *E. coli* is indeed capable of improving its growth
270 with pCbl via genetic changes, and it uses differing strategies depending on the availability of the
271 nutrient. Competition experiments and genetic analyses revealed regulation of corrinoid uptake as
272 a limiting factor in *E. coli* and a previously unappreciated role for the corrinoid adenosyltransferase
273 BtuR in MetH-dependent growth.

274 We previously showed that the cobamide-dependent enzyme methylmalonyl-CoA mutase
275 (MCM) has different binding affinities for different cobamides, and that these cobamide-binding
276 affinities largely mirror MCM-dependent growth with different cobamides in *Sinorhizobium*
277 *meliloti* (13). Other studies have shown that MetH orthologs from different organisms display
278 distinct preferences for different cobamides (9, 14, 25). Given that pCbl is less preferred by *E. coli*
279 than Cbl (Fig. 1B), we hypothesized that passaging with pCbl would lead to the accumulation of
280 mutations in the MetH enzyme that improved its ability to bind and use pCbl. Though we observed
281 mutations that presumably impact *metH* expression, no mutations were found in the *metH* coding
282 sequence. Altering expression of corrinoid-related genes was the general outcome of our evolution
283 experiment, suggesting that modifying the regulation of cobamide metabolism may be a more
284 readily accessible mechanism of adaptation than changes to the specificity of the dependent
285 enzyme, particularly in our experimental timeframe. Changes to gene expression are routinely seen
286 in laboratory evolution experiments, including the targeting of global regulators (39, 40).

287 While mutations in *metH* and its transcriptional activator *metR* were found at the higher
288 concentration of pCbl, mutations upregulating the outer membrane corrinoid transporter BtuB
289 arose primarily when pCbl was limiting, consistent with its role in corrinoid uptake. Indeed, we
290 previously showed that overexpression of the corrinoid transport machinery in *Bacillus subtilis*
291 increases the amount of cobamide imported (32). Although it is not known whether the affinity of
292 BtuB for Cbl versus pCbl differs, structural and biochemical studies with Cbl and a corrinoid
293 intermediate lacking a lower ligand (cobinamide) have shown that the lower ligand is of minimal
294 importance to binding, with BtuB primarily interacting with the corrin moiety (41-43). Instead,
295 greater *btuB* expression, leading to increased pCbl uptake, could compensate for decreased MetH
296 efficiency with pCbl at a later step such as adenosylation by BtuR or utilization by MetH.
297 Alternatively, the evolved mutations upregulating *btuB* may also be a consequence of the selective
298 pressure from competing for limiting pCbl. Cobamide uptake is critical for colonization by the
299 human gut commensal bacterium *Bacteroides thetaiotaomicron* in a mouse model (44), and *B.*
300 *thetaiotaomicron* and other *Bacteroides* species encode multiple corrinoid transport systems which
301 include high-affinity corrinoid binding proteins absent from *E. coli* (45). These uptake systems are
302 thought to enable *Bacteroides* to outcompete other microbes for corrinoids, allowing for successful
303 gut colonization (46, 47). Our observation that corrinoid uptake and competitiveness in *E. coli* can
304 readily be improved via mutations in the *btuB* promoter or RBS suggests that *E. coli* is not evolved
305 to maximize corrinoid uptake, despite its being a member of the gut microbiota like *B.*
306 *thetaiotaomicron*. This is notable given that the purinyl cobamides, which include pCbl, were
307 found to be the dominant fecal corrinoids in the majority of human subjects (5). *E. coli* could be
308 under less selective pressure to maximize corrinoid uptake because, unlike *B. thetaiotaomicron*,
309 *E. coli* has the cobamide-independent methionine synthase *metE* as well as *metH*, rendering it less

310 dependent on exogenous cobamides. In addition, BtuB is a phage receptor in *E. coli*, so increased
311 expression of *btuB* may not always be beneficial in natural settings (48).

312 The BtuR corrinoid adenosyltransferase is responsible for installing a 5′-deoxyadenosine
313 moiety as the β ligand of cobamides to produce adenosylcobamides (49), which are required for
314 the subset of cobamide-dependent enzymes, such as MCM, that carry out radical-based reactions
315 (50). However, no role for adenosylcobamides has been proposed for methyltransferases such as
316 MetH, which use methylcobamides – cobamides with a methyl group as the β ligand – to shuttle
317 methyl groups from a methyl donor to a substrate. Therefore, it was surprising to find that, in
318 MetH-dependent *E. coli*, overexpression of *btuR* provides a competitive advantage during growth
319 with pCbl, deletion of *btuR* impairs growth with both pCbl and Cbl, and supplementation of the
320 Δ*btuR* mutant with adenosylcobamides only partially rescues the growth phenotype. These results
321 suggest that adenosylcobamides, and perhaps the BtuR protein itself, could have previously
322 unknown roles in MetH function. Some cobamide-dependent enzymes such as MCM require a
323 corrinoid adenosyltransferase and other accessory proteins to load the cobamide cofactor into the
324 enzyme (51-53). It is possible that BtuR fulfills such a role for MetH in *E. coli*, particularly for
325 cobamides that function poorly as a cofactor for MetH. Alternatively, adenosylcobamides and/or
326 BtuR could facilitate SAM-dependent cobamide reactivation, a step required approximately every
327 2,000 turnovers for Cbl following spontaneous cofactor oxidation (54-56). Until recently, studies
328 of *E. coli* MetH have been unable to address the cofactor loading step because the enzyme is stable
329 only when pre-loaded with Cbl during purification. Future *in vitro* studies with a newly identified
330 MetH homolog that is stable in its apo form will facilitate analysis of this phase of the reaction
331 (57). Because pCbl functions more poorly than Cbl in *E. coli* MetH-dependent growth, our
332 evolution experiment may have fortuitously uncovered a role for adenosylated cobamides in
333 corrinoid-dependent physiology. Future work will be aimed at understanding the molecular
334 mechanisms underlying these observations.

335 **Material and Methods**

336 *Media and growth conditions*

337 *E. coli* MG1655 Δ*metE* evolution was performed at 37°C with aeration in M9 glycerol
338 (0.2%) minimal medium (58) with the indicated concentrations of pCbl. 20 ml cultures were grown
339 in glass test tubes with 0.2 ml transferred into fresh media every 24 hours. A sample of each
340 population was archived on days 14, 28, 51, 65, 84, 98, and 104 in 25% glycerol and stored at -
341 80°C. Before the start of the evolution experiment, the three replicate cultures were passaged daily
342 for 16 days with a saturating level of pCbl (5 or 2.5 nM) while the appropriate concentrations for
343 the evolution experiment were being determined.

344 M9 medium was supplemented with L-methionine (Met) at 0.1 mg/ml unless indicated.
345 LB agar was used as solid medium. For experiments with the *E. coli* Δ*metE* ancestor or evolved
346 isolates from Culture 8, M9 medium was inoculated with individual colonies grown on LB agar.
347 Pre-culturing of populations and strains in M9 medium was performed at 37°C with aeration.

348 *Strain construction*

349 All strains used for evolution and mutant validation are derivatives of wild type K12 strain
350 MG1655. *E. coli* strains were cultured at 37°C with aeration in LB medium during strain
351 construction. Media were supplemented with antibiotics at the following concentrations when
352 necessary: kanamycin, 25 mg/liter (pKIKO, pETmini); carbenicillin, 100 mg/liter (pCP20);
353 chloramphenicol, 10-20 mg/liter (pACYCDuet-1). pKIKO*arsB*Km plasmids were propagated in
354 *E. coli* DH5α containing λ*pir*.

355 The Δ*metE*::kan^R and Δ*btuR*::kan^R mutations from the Keio collection (59) were
356 introduced by P1 transduction into *E. coli* strain MG1655 (59, 60). The kanamycin resistance
357 cassette was removed from Δ*metE*::kan^R by introducing the plasmid pCP20 as described, leaving
358 the FRT site in place of the *metE* coding sequence (61).

359 An *E. coli* strain overexpressing *btuB* was created by integrating an additional copy of *btuB*
360 at the *arsB* (arsenite transporter) locus using the KIKO system as described (62). pKIKO*arsB*Km
361 was a gift from Lars Nielsen & Claudia Vickers (Addgene plasmid # 46766;
362 http://n2t.net/addgene:46766; RRID:Addgene_46766). *E. coli btuB* with its promoter and
363 riboswitch was cloned into pKIKO*arsB*Km, with the promoter containing the -35 element
364 mutation (TTGACA) found in evolved populations and isolates. *btuB* also contained a
365 synonymous mutation in codon 581 encoding a valine (GTT to GTA). The PCR-based method
366 was used to integrate this construct at the *arsB* locus. The kanamycin resistance cassette alone
367 from pKIKO*arsB*Km was integrated at the *arsB* locus to create a control strain. Both constructs
368 were first integrated into MG1655 before being transduced via P1 into the Δ*metE* strain. Finally,
369 the kanamycin resistance cassette was removed using pCP20. Strains were confirmed by PCR and
370 Sanger sequencing. Plasmids pSG013 and pSG015, which contain mCerulean and mCitrine
371 (abbreviated CFP and YFP in text), respectively, were each transformed into the two strains to
372 enable tracking based on fluorescence (63).

373 The *btuR* and *yciK* genes were overexpressed in a pACYCDuet-1 plasmid in which the T7
374 promoters were replaced with a *lac* promoter and operator (pACYCDuet-1-pLac). This enabled
375 repression of gene expression in the presence of glucose (0.02% in LB, 0.2% in M9) and
376 expression in the absence of glucose due to the leakiness of the *lac* promoter. *E. coli btuR*, *yciK*,
377 and the *yciK-btuR* operon were each cloned downstream of the *lac* promoter in pACYCDuet-1-
378 pLac. mCerulean and mCitrine genes from pSG013 and pSG015 (with J23100 promoter and
379 B0034 RBS) were inserted between the chloramphenicol resistance cassette and p15A origin in
380 each of these plasmid constructs to enable tracking of strains by fluorescence measurements (63).

381 *Cobamide reagents*

382 CNCbl and AdoCbl were purchased from MilliporeSigma. CNpCbl was extracted from
383 *Propionibacterium acidi-propionici* strain DSM 20273 and purified as described (64, 65).
384 AdopCbl was chemically synthesized from CNpCbl and purified as described (13). Cobamides
385 were quantified spectrophotometrically (13, 26). Cbl and pCbl were used in their cyano forms
386 (CNCbl and CNpCbl) unless otherwise indicated.

387 *Growth assays and competition experiments*

388 To quantify the percentage of small colonies present during the evolution of Culture 8,
389 archived populations were cultured overnight in M9 glycerol medium supplemented with 0.35 nM
390 pCbl, diluted, and plated on LB agar.

391 Growth assays and competition experiments were performed in 200 µl cultures in 96-well
392 plates (Corning, 3598). For growth curves, populations or isolates were pre-cultured in M9
393 glycerol supplemented with 0.35 nM pCbl, while cultures for cobamide dose-response assays were
394 supplemented with Met. Cells from saturated cultures were collected by centrifugation,
395 resuspended in M9 glycerol, and OD_{600} was measured. Each culture was then inoculated at a
396 starting OD_{600} of 0.01 in M9 glycerol medium with the indicated supplement. 96-well plates were
397 sealed with Breathe-Easy (Diversified Biotech). Growth assays were performed in a BioTek
398 Synergy 2 microplate reader with shaking at medium speed at 37°C and OD_{600} recorded every 15
399 min for 24 hours. OD_{600} for cobamide dose-response assays was measured with the BioTek
400 Synergy 2 microplate reader following 22 h growth at 37°C with shaking in either the plate reader
401 or a heated benchtop microplate shaker (1,200 rpm, Southwest Science). Preparation of cultures
402 containing adenosylcobamides was done under red light and the plates were incubated in the dark.
403 EC_{50} values were calculated using Graphpad Prism (Dose-response – Stimulation; [Agonist] vs.
404 response – Variable slope (four parameters)).

405 For competition experiments involving evolved populations or strains, cells were pre-
406 cultured in M9 glycerol medium supplemented with Met. Cells were pelleted, washed twice with
407 0.85% saline, and resuspended in M9 glycerol medium, with the exception of the experiments
408 shown in Fig. 2C and 3D, in which the cells were pelleted and resuspended in M9 glycerol medium
409 without washing. OD_{600} was measured and the population or an equal ratio of two strains was
410 inoculated at a starting OD_{600} of 0.01 in 200 µl M9 glycerol medium containing the indicated
411 supplement. A dilution of the culture was plated on LB agar to establish the percentage of small
412 colonies at time 0. The plate was sealed and incubated at 37°C in a benchtop microplate shaker at
413 1,200 rpm. 2 µl of each culture was transferred into 198 µl fresh medium every 24 h. On the
414 indicated days, dilutions from the cultures were plated on LB agar to determine the percentage of
415 small colonies in the population.

416 Competition experiments involving *btuB*-overexpression strains were tracked by
417 fluorescence (63). Strains were pre-cultured in M9 glycerol medium supplemented with Met. Cells
418 were pelleted, washed twice with 0.85% saline, and resuspended in M9 glycerol medium. OD_{600}
419 was measured and each sample was adjusted to an OD_{600} of 0.25. Co-cultures were prepared by
420 mixing an equal volume of each strain. 100 µl of each co-culture was transferred to a 96-well glass
421 bottom plate (P96-1.5P, Cellvis) and cyan and yellow fluorescence were measured on a multiwell
422 plate reader (Tecan Spark) as described (63). Separately, 8 µl of each mono- and co-culture were
423 added to 192 µl of M9 glycerol medium (starting OD_{600} of 0.01) containing the specified
424 amendment in 96-well plates. Plates were sealed and incubated at 37°C in a benchtop microplate
425 shaker (1,200 rpm). 2 µl of each culture was transferred into 198 µl fresh medium every 24 h. At
426 the specified timepoints, aliquots were diluted in M9 medium and CFP and YFP values were
427 measured. Standard curves for conversion of fluorescence to OD_{600} equivalents were generated
428 from saturated cultures grown in tubes (for t = 0 readings only) or mono-culture controls grown in
429 96-well plates (from t = 1 day on). Competition experiments with pACYCDuet-1-pLac plasmids

430 expressing *btuR* and/or *yciK* were performed similarly except that strains were pre-cultured in M9
431 glucose (0.2%) medium with Met.

432 *Whole genome sequencing and analysis*

433 Evolved populations were grown in M9 medium supplemented with 0.35 nM pCbl, while
434 evolved isolates and the Δ*metE* ancestor were cultured in M9 medium supplemented with Met.
435 Genomic DNA was isolated with a DNeasy Blood and Tissue Kit (Qiagen) and submitted to
436 Novogene (Sacramento, CA, USA) for library preparation and whole genome sequencing using
437 an Illumina NovaSeq 6000.

438 Identification of mutations was performed by Novogene by comparison to the *E. coli*
439 MG1655 reference genome (accession PRJNA57779). SNPs and InDels were detected using
440 SAMtools with the parameter 'mpileup -m 2 -F 0.002 -d 1000' and annotated using ANNOVAR
441 (66, 67). The results were filtered such that the number of support reads for each SNP/InDel was
442 greater than 4 and the mapping quality of each SNP/InDel was higher than 20. SVs were detected
443 by BreakDancer and annotated by ANNOVAR (68). SVs were filtered by removing those with
444 fewer than 2 supporting PE reads. A comparison to the Δ*metE* ancestor was made to eliminate
445 mutations in the genome present prior to the laboratory evolution.

446 *Measurement of* btuB *and* btuR *expression in evolved isolates by RT-qPCR*

447 The *E. coli* Δ*metE* ancestor and evolved isolates S2, S3, S4, R1, and R3 were streaked onto
448 LB agar and grown at 37°C. Three individual colonies of each strain were inoculated into M9
449 glycerol medium supplemented with 1 nM pCbl. After 22 hours of growth at 37°C, the cultures
450 were passaged into fresh medium at an OD_{600} of 0.01 and grown for 20 hours. Cultures were then
451 diluted to an OD_{600} of 0.03 in fresh medium and samples were collected during exponential phase
452 (OD_{600} ~0.4). 875 µl of each culture was mixed with 1.75 ml RNAprotect® Bacteria Reagent and
453 RNA was extracted with the RNeasy Mini Kit (Qiagen). On-column DNase digestion was
454 performed to remove DNA. RNA was quantified using a Qubit fluorometer (Invitrogen). 100 ng
455 of RNA was used to synthesize cDNA in 20 µl reactions with iScript RT Supermix (Biorad). 5 µl
456 of 50-fold diluted cDNA was used in 20 µl reactions with SsoAdvanced Universal SYBR Green
457 Supermix (Biorad), with reactions performed in triplicate with each primer pair (5 µM). qPCR was
458 performed on a CFX96 Touch Real-Time PCR Detection System (Biorad) with the following
459 conditions: one cycle of denaturation at 95°C for 3 min, and 40 cycles of denaturation at 95°C for
460 10 sec and extension at 59°C for 30 sec. C_q values were normalized against previously reported
461 reference genes *mdh* and *rpoA* (69) and relative gene expression was calculated using the $\Delta\Delta C_q$
462 method. Primers used for qPCR are listed in Table S2.

463 *Corrinoid bioassay to assess cobamide uptake and retention*

464 *E. coli* Δ*btuR* Δ*metE* and Δ*metE* strains were pre-cultured in M9 glycerol medium
465 supplemented with Met. The strains were then inoculated at an OD_{600} of 0.01 in 1 ml M9 glycerol
466 medium supplemented with AdopCbl, CNpCbl, AdoCbl, or CNCbl. The medium was also
467 supplemented with 0.02 mg/ml Met, a concentration that ensured saturating growth of the pCbl
468 cultures but did not affect growth of the Δ*metE* strain in the subsequent bioassay. Cultures were
469 incubated at 37°C with aeration for 22 hours. Cultures containing adenosylcobamides were

470 prepared under red light and incubated in the dark. 750 µl of each culture was centrifuged for 5
471 min at 6,000 x g to pellet cells. 600 µl of the supernatant was passed through a 0.22 µm filter. The
472 cell pellet was washed twice with 0.85% saline and resuspended in 750 µl saline. All samples were
473 then incubated at 100°C for 20 min. Samples containing the pellet fraction were centrifuged for 5
474 min at 6,000 x g and 600 µl of supernatant was removed to use as the cell lysate. The *E. coli*
475 bioassay was performed in 96 well plates as described (65), except M9 glycerol was used as the
476 growth medium and plates were incubated at 37°C in a microplate shaker for 22 hours prior to
477 measurement of OD_{600}. The concentration of cobamides in each sample was determined using
478 standard curves generated with CNpCbl and CNCbl.

479 *Corrinoid extraction and analysis*

480 *E. coli* Δ*btuR* Δ*metE* was pre-cultured in M9 glycerol medium supplemented with Met.
481 OD_{600} was measured and cells were inoculated into 250 ml M9 glycerol medium containing 1 nM
482 pCbl or Cbl at an OD_{600} of 0.01. The medium with 1 nM pCbl was supplemented with Met to
483 enable growth of *E. coli* Δ*btuR* Δ*metE*. Cultures were grown at 37°C with aeration for 22 h. Cells
484 were collected by centrifugation and washed twice with saline. Corrinoids were extracted with
485 KCN as described (65). Extractions were analyzed on an Agilent Zorbax SB-Aq column (5 µm,
486 4.6 x 150 mm) with an Agilent 1200 series HPLC equipped with a diode array detector using
487 Method 2 (10). Cobamides in each sample were quantified using standard curves generated with
488 CNpCbl and CNCbl.

489 **Acknowledgements**

490 We thank Alexa Nicolas for advice on whole genome sequencing and analysis, Sophia
491 Adler for advice with RT-qPCR, Zoila Alvarez-Aponte, Markos Koutmos and members of the
492 Taga Lab for helpful discussions, and Janani Hariharan, Dennis Suazo, and Eleanor Wang for
493 critical reading of the manuscript. We are grateful to Olga Sokolovskaya for synthesis of AdopCbl
494 and Sebastian Gude for construction of pSG013 and pSG015. This work was funded by National
495 Institutes of Health grants R35GM139633 to M.E.T. and 5K99GM143653-02 to Z.F.H. R.R.P.
496 was supported by the NIH T32GM132022 training grant.

497 **References**

498 1. Sokolovskaya OM, Shelton AN, Taga ME. 2020. Sharing vitamins: Cobamides unveil microbial
499 interactions. Science 369:eaba0165.
500 2. Roth JR, Lawrence JG, Bobik TA. 1996. Cobalamin (coenzyme B_{12}): synthesis and biological
501 significance. Annu Rev of Microbiol 50:137-181.
502 3. Shelton AN, Seth EC, Mok KC, Han AW, Jackson SN, Haft DR, Taga ME. 2019. Uneven
503 distribution of cobamide biosynthesis and dependence in bacteria predicted by comparative
504 genomics. ISME J 13:789-804.
505 4. Huemer M, Baumgartner MR. 2019. The clinical presentation of cobalamin-related disorders: From
506 acquired deficiencies to inborn errors of absorption and intracellular pathways. J Inherit Metab Dis
507 42:686-705.
508 5. Allen RH, Stabler SP. 2008. Identification and quantitation of cobalamin and cobalamin analogues
509 in human feces. Am J Clin Nutr 87:1324-35.

510 6. Yan J, Bi M, Bourdon AK, Farmer AT, Wang PH, Molenda O, Quaile AT, Jiang N, Yang Y, Yin
511 Y, Simsir B, Campagna SR, Edwards EA, Loffler FE. 2018. Purinyl-cobamide is a native prosthetic
512 group of reductive dehalogenases. Nat Chem Biol 14:8-14.
513 7. Renz P. 1999. Biosynthesis of the 5,6-dimethylbenzimidazole moiety of cobalamin and of the other
514 bases found in natural corrinoids, p 557-566. *In* Banerjee R (ed), Chemistry and Biochemistry of
515 B12. John Wiley & Sons, Inc., New York.
516 8. Ma AT, Beld J, Brahamsha B. 2017. An amoebal grazer of cyanobacteria requires cobalamin
517 produced by heterotrophic bacteria. Appl and Environ Microbiol 83:e00035-17.
518 9. Ma AT, Tyrell B, Beld J. 2020. Specificity of cobamide remodeling, uptake and utilization in *Vibrio*
519 *cholerae*. Mol Microbiol 113:89-102.
520 10. Mok KC, Taga ME. 2013. Growth inhibition of *Sporomusa ovata* by incorporation of
521 benzimidazole bases into cobamides. J Bacteriol 195:1902-11.
522 11. Schubert T, von Reuss SH, Kunze C, Paetz C, Kruse S, Brand-Schon P, Nelly AM, Nuske J, Diekert
523 G. 2019. Guided cobamide biosynthesis for heterologous production of reductive dehalogenases.
524 Microb Biotechnol 12:346-359.
525 12. Shelton AN, Lyu X, Taga ME. 2020. Flexible Cobamide Metabolism in *Clostridioides*
526 (*Clostridium*) *difficile* 630 Δ*erm*. J Bacteriol 202.
527 13. Sokolovskaya OM, Mok KC, Park JD, Tran JLA, Quanstrom KA, Taga ME. 2019. Cofactor
528 Selectivity in Methylmalonyl Coenzyme A Mutase, a Model Cobamide-Dependent Enzyme. mBio
529 10:e01303-19.
530 14. Tanioka Y, Miyamoto E, Yabuta Y, Ohnishi K, Fujita T, Yamaji R, Misono H, Shigeoka S, Nakano
531 Y, Inui H, Watanabe F. 2010. Methyladeninylcobamide functions as the cofactor of methionine
532 synthase in a cyanobacterium, *Spirulina platensis* NIES-39. FEBS Lett 584:3223-6.
533 15. Watanabe F, Nakano Y, Stupperich E. 1992. Different corrinoid specificities for cell growth and
534 cobalamin uptake in *Euglena gracilis* Z. J Gen Microbiol 138:1807-1813.
535 16. Hallberg ZF, Seth EC, Thevasundaram K, Taga ME. 2022. Comparative Analysis of Corrinoid
536 Profiles across Host-Associated and Environmental Samples. Biochemistry 61:2791-2796.
537 17. Men Y, Seth EC, Yi S, Crofts TS, Allen RH, Taga ME, Alvarez-Cohen L. 2015. Identification of
538 specific corrinoids reveals corrinoid modification in dechlorinating microbial communities.
539 Environ Microbiol 17:4873-84.
540 18. Wienhausen G, Dlugosch L, Jarling R, Wilkes H, Giebel HA, Simon M. 2022. Availability of
541 vitamin B_{12} and its lower ligand intermediate α-ribazole impact prokaryotic and protist
542 communities in oceanic systems. ISME J 16:2002-2014.
543 19. Kelly CJ, Alexeev EE, Farb L, Vickery TW, Zheng L, Eric LC, Kitzenberg DA, Battista KD,
544 Kominsky DJ, Robertson CE, Frank DN, Stabler SP, Colgan SP. 2019. Oral vitamin B_{12} supplement
545 is delivered to the distal gut, altering the corrinoid profile and selectively depleting *Bacteroides* in
546 C57BL/6 mice. Gut Microbes 10:654-662.
547 20. Xu Y, Xiang S, Ye K, Zheng Y, Feng X, Zhu X, Chen J, Chen Y. 2018. Cobalamin (Vitamin B12)
548 Induced a Shift in Microbial Composition and Metabolic Activity in an *in vitro* Colon Simulation.
549 Front Microbiol 9:2780.
550 21. Zhu X, Xiang S, Feng X, Wang H, Tian S, Xu Y, Shi L, Yang L, Li M, Shen Y, Chen J, Chen Y,
551 Han J. 2019. Impact of Cyanocobalamin and Methylcobalamin on Inflammatory Bowel Disease
552 and the Intestinal Microbiota Composition. J Agric Food Chem 67:916-926.
553 22. Hallberg ZF, Nicolas AM, Alvarez-Aponte ZI, Mok KC, Sieradzki ET, Pett-Ridge J, Banfield JF,
554 Carlson HK, Firestone MK, Taga ME. 2024. Soil microbial community response to corrinoids is
555 shaped by a natural reservoir of vitamin B_{12}. ISME J doi:10.1093/ismejo/wrae094.
556 23. Gray MJ, Escalante-Semerena JC. 2009. The cobinamide amidohydrolase (cobyric acid-forming)
557 CbiZ enzyme: a critical activity of the cobamide remodelling system of *Rhodobacter sphaeroides*.
558 Mol Microbiol 74:1198-210.

559 24. Yi S, Seth EC, Men YJ, Stabler SP, Allen RH, Alvarez-Cohen L, Taga ME. 2012. Versatility in
560 corrinoid salvaging and remodeling pathways supports corrinoid-dependent metabolism in
561 *Dehalococcoides mccartyi*. Appl Environ Microbiol 78:7745-52.
562 25. Helliwell KE, Lawrence AD, Holzer A, Kudahl UJ, Sasso S, Kräutler B, Scanlan DJ, Warren MJ,
563 Smith AG. 2016. Cyanobacteria and Eukaryotic Algae Use Different Chemical Variants of Vitamin
564 B_{12}. Curr Biol 26:999-1008.
565 26. Mok KC, Sokolovskaya OM, Nicolas AM, Hallberg ZF, Deutschbauer A, Carlson HK, Taga ME.
566 2020. Identification of a Novel Cobamide Remodeling Enzyme in the Beneficial Human Gut
567 Bacterium *Akkermansia muciniphila*. mBio 11.
568 27. Stupperich E, Steiner I, Eisinger HJ. 1987. Substitution of Coα-(5-
569 Hydroxybenzimidazolyl)Cobamide (Factor III) by Vitamin B_{12} in *Methanobacterium*
570 *thermoautotrophicum*. J Bacteriol 169:3076-81.
571 28. Rodionov DA, Vitreschak AG, Mironov AA, Gelfand MS. 2003. Comparative genomics of the
572 Vitamin B_{12} metabolism and regulation in prokaryotes. J Biol Chem 278:41148-59.
573 29. Winkler WC, Breaker RR. 2005. Regulation of bacterial gene expression by riboswitches. Annu
574 Rev Microbiol 59:487-517.
575 30. McCown PJ, Corbino KA, Stav S, Sherlock ME, Breaker RR. 2017. Riboswitch diversity and
576 distribution. RNA 23:995-1011.
577 31. Nahvi A, Sudarsan N, Ebert MS, Zou X, Brown KL, Breaker RR. 2002. Genetic control by a
578 metabolite binding mRNA. Chem Biol 9:1043.
579 32. Kennedy KJ, Widner FJ, Sokolovskaya OM, Innocent LV, Procknow RR, Mok KC, Taga ME.
580 2022. Cobalamin Riboswitches Are Broadly Sensitive to Corrinoid Cofactors to Enable an Efficient
581 Gene Regulatory Strategy. mBio 13:e0112122.
582 33. Rozen DE, Lenski RE. 2000. Long-Term Experimental Evolution in *Escherichia coli*. VIII.
583 Dynamics of a Balanced Polymorphism. Am Nat 155:24-35.
584 34. Ching C, Zaman MH. 2020. Development and selection of low-level multi-drug resistance over an
585 extended range of sub-inhibitory ciprofloxacin concentrations in *Escherichia coli*. Sci Rep
586 10:8754.
587 35. Urbanowski ML, Stauffer LT, Plamann LS, Stauffer GV. 1987. A new methionine locus, *metR*,
588 that encodes a trans-acting protein required for activation of *metE* and *metH* in *Escherichia coli*
589 and *Salmonella typhimurium*. J Bacteriol 169:1391-7.
590 36. Marconi R, Wigboldus J, Weissbach H, Brot N. 1991. Transcriptional start and MetR binding sites
591 on the *Escherichia coli metH* gene. Biochem Biophys Res Commun 175:1057-63.
592 37. Punekar AS, Porter J, Carr SB, Phillips SE. 2016. Structural basis for DNA recognition by the
593 transcription regulator MetR. Acta Crystallogr F Struct Biol Commun 72:417-26.
594 38. Doublet P, van Heijenoort J, Bohin JP, Mengin-Lecreulx D. 1993. The *murI* gene of *Escherichia*
595 *coli* is an essential gene that encodes a glutamate racemase activity. J Bacteriol 175:2970-9.
596 39. Dragosits M, Mattanovich D. 2013. Adaptive laboratory evolution - principles and applications for
597 biotechnology. Microb Cell Fact 12:64.
598 40. Conrad TM, Lewis NE, Palsson BO. 2011. Microbial laboratory evolution in the era of genome-
599 scale science. Mol Syst Biol 7:509.
600 41. Bradbeer C, Gudmundsdottir A. 1990. Interdependence of calcium and cobalamin binding by wild-
601 type and mutant BtuB protein in the outer membrane of *Escherichia coli*. J Bacteriol 172:4919-26.
602 42. Chimento DP, Kadner RJ, Wiener MC. 2003. The *Escherichia coli* outer membrane cobalamin
603 transporter BtuB: structural analysis of calcium and substrate binding, and identification of
604 orthologous transporters by sequence/structure conservation. J Mol Biol 332:999-1014.
605 43. Kenley JS, Leighton M, Bradbeer C. 1978. Transport of vitamin B_{12} in *Escherichia coli*. Corrinoid
606 specificity of the outer membrane receptor. J Biol Chem 253:1341-6.
607 44. Goodman AL, McNulty NP, Zhao Y, Leip D, Mitra RD, Lozupone CA, Knight R, Gordon JI. 2009.
608 Identifying genetic determinants needed to establish a human gut symbiont in its habitat. Cell Host
609 Microbe 6:279-89.

610 45. Degnan PH, Barry NA, Mok KC, Taga ME, Goodman AL. 2014. Human gut microbes use multiple
611 transporters to distinguish vitamin B_{12} analogs and compete in the gut. Cell Host Microbe 15:47-
612 57.
613 46. Putnam EE, Abellon-Ruiz J, Killinger BJ, Rosnow JJ, Wexler AG, Folta-Stogniew E, Wright AT,
614 van den Berg B, Goodman AL. 2022. Gut Commensal *Bacteroidetes* Encode a Novel Class of
615 Vitamin B_{12}-Binding Proteins. mBio 13:e0284521.
616 47. Wexler AG, Schofield WB, Degnan PH, Folta-Stogniew E, Barry NA, Goodman AL. 2018. Human
617 gut *Bacteroides* capture vitamin B_{12} via cell surface-exposed lipoproteins. Elife 7.
618 48. Bradbeer C, Woodrow ML, Khalifah LI. 1976. Transport of vitamin B_{12} in *Escherichia coli*:
619 common receptor system for vitamin B_{12} and bacteriophage BF23 on the outer membrane of the
620 cell envelope. J Bacteriol 125:1032-9.
621 49. Escalante-Semerena JC. 2007. Conversion of cobinamide into adenosylcobamide in bacteria and
622 archaea. J Bacteriol 189:4555-60.
623 50. Banerjee R, Ragsdale SW. 2003. The many faces of vitamin B_{12}: catalysis by cobalamin-dependent
624 enzymes. Annu Rev Biochem 72:209-47.
625 51. Padovani D, Banerjee R. 2009. A G-protein editor gates coenzyme B_{12} loading and is corrupted in
626 methylmalonic aciduria. Proc Natl Acad Sci U S A 106:21567-72.
627 52. Padovani D, Labunska T, Palfey BA, Ballou DP, Banerjee R. 2008. Adenosyltransferase tailors
628 and delivers coenzyme B_{12}. Nat Chem Biol 4:194-6.
629 53. Takahashi-Iniguez T, Gonzalez-Noriega A, Michalak C, Flores ME. 2017. Human MMAA induces
630 the release of inactive cofactor and restores methylmalonyl-CoA mutase activity through their
631 complex formation. Biochimie 142:191-196.
632 54. Datta S, Koutmos M, Pattridge KA, Ludwig ML, Matthews RG. 2008. A disulfide-stabilized
633 conformer of methionine synthase reveals an unexpected role for the histidine ligand of the
634 cobalamin cofactor. Proc Natl Acad Sci U S A 105:4115-20.
635 55. Fujii K, Huennekens FM. 1974. Activation of methionine synthetase by a reduced
636 triphosphopyridine nucleotide-dependent flavoprotein system. J Biol Chem 249:6745-53.
637 56. Jarrett JT, Huang S, Matthews RG. 1998. Methionine synthase exists in two distinct conformations
638 that differ in reactivity toward methyltetrahydrofolate, adenosylmethionine, and flavodoxin.
639 Biochemistry 37:5372-82.
640 57. Mendoza J, Purchal M, Yamada K, Koutmos M. 2023. Structure of full-length cobalamin-
641 dependent methionine synthase and cofactor loading captured in crystallo. Nat Commun 14:6365.
642 58. Sambrook J. 2001. Molecular cloning : a laboratory manual. Cold Spring Harbor Laboratory Press,
643 Cold Spring Harbor, N.Y.
644 59. Baba T, Ara T, Hasegawa M, Takai Y, Okumura Y, Baba M, Datsenko KA, Tomita M, Wanner
645 BL, Mori H. 2006. Construction of *Escherichia coli* K-12 in-frame, single-gene knockout mutants:
646 the Keio collection. Mol Syst Biol 2:0008.
647 60. Silhavy TJ, Berman ML, Enquist LW. 1984. Experiments with Gene Fusions. Cold Spring Harbor
648 Laboratory Press, Cold Spring Harbor, NY.
649 61. Datsenko KA, Wanner BL. 2000. One-step inactivation of chromosomal genes in *Escherichia coli*
650 K-12 using PCR products. Proc Natl Acad Sci U S A 97:6640-5.
651 62. Sabri S, Steen JA, Bongers M, Nielsen LK, Vickers CE. 2013. Knock-in/Knock-out (KIKO)
652 vectors for rapid integration of large DNA sequences, including whole metabolic pathways, onto
653 the *Escherichia coli* chromosome at well-characterised loci. Microb Cell Fact 12:60.
654 63. Gude S, Pherribo GJ, Taga ME. 2022. A Salvaging Strategy Enables Stable Metabolite
655 Provisioning among Free-Living Bacteria. mSystems 7:e0028822.
656 64. Hoffmann B, Oberhuber M, Stupperich E, Bothe H, Buckel W, Konrat R, Kräutler B. 2000. Native
657 corrinoids from *Clostridium cochlearium* are adeninylcobamides: Spectroscopic analysis and
658 identification of pseudovitamin B_{12} and factor A. J Bacteriol 182:4773-82.
659 65. Mok KC, Hallberg ZF, Taga ME. 2022. Purification and detection of vitamin B_{12} analogs. Methods
660 Enzymol 668:61-85.

661 66. Li H, Handsaker B, Wysoker A, Fennell T, Ruan J, Homer N, Marth G, Abecasis G, Durbin R,
662 Subgroup GPDP. 2009. The Sequence Alignment/Map format and SAMtools. Bioinformatics
663 25:2078-9.
664 67. Wang K, Li M, Hakonarson H. 2010. ANNOVAR: functional annotation of genetic variants from
665 high-throughput sequencing data. Nucleic Acids Res 38:e164.
666 68. Chen K, Wallis JW, McLellan MD, Larson DE, Kalicki JM, Pohl CS, McGrath SD, Wendl MC,
667 Zhang Q, Locke DP, Shi X, Fulton RS, Ley TJ, Wilson RK, Ding L, Mardis ER. 2009.
668 BreakDancer: an algorithm for high-resolution mapping of genomic structural variation. Nat
669 Methods 6:677-81.
670 69. Pons MC, Praud K, Da Re S, Cloeckaert A, Doublet B. 2023. Conjugative IncC Plasmid Entry
671 Triggers the SOS Response and Promotes Effective Transfer of the Integrative Antibiotic
672 Resistance Element SGI1. Microbiol Spectr 11:e0220122.

673